

Research article

Analysis and optimization of electrospinning parameters for fabricating thermoplastic polyurethanes (TPU) nanofibers by response surface methodology

Lu Liu^{ID}, Tian Luo^{ID}, Xiaoju Kuang^{ID}, Xiaoqian Wan^{ID}, Xinhua Liang^{ID}, Gaoming Jiang^{ID}, Honglian Cong^{ID}, Haijun He^{*ID}

Engineering Research Center for Knitting Technology, Ministry of Education, Jiangnan University, 214122 Wuxi, China

Received 3 April 2024; accepted in revised form 22 May 2024

Abstract. Thermoplastic polyurethanes (TPU) have attracted increasing attention due to their excellent flexibility, chemical stability, processability and greenness. The traditional processes generally limit them to civil and industrial applications, but electrospun TPU nanofibers with high porosity, high specific surface area and superior mechanical properties are promising in emerging fields. TPU nanofibers' properties are affected by various electrospinning parameters, such as solution concentration, applied voltage, flow rate and rotational speed. Thus, 29 sets of experiments were designed here by the efficient and low-cost response surface methodology (RSM). The analysis of variance (ANOVA) revealed that the model agrees well with experimental results, and solution concentration is the most crucial parameter affecting nanofibers' morphology and diameter. Based on it, the impacts of solution concentration and orientation on the mechanical properties of the TPU nanofiber membrane were investigated. Benefiting from the stress transfer and network deformation, the TPU nanofiber membranes parallel to the collection direction possessed the highest stress strength (23.71 MPa), while the nanofiber membranes vertical showed the widest strain range (485%). This study provides useful guidance for the preparation of high-performance TPU nanofibers, contributing to expanding its applicability in emerging fields such as biomedical, filtration and separation, and flexible sensing.

Keywords: TPU nanofibers, electrospinning parameters, response surface methodology, mechanical properties, orientation of nanofibers

1. Introduction

Owing to the combination of rubber elasticity and plasticity, thermoplastic polyurethanes (TPU) are known as the “Third Generation Rubber” after natural rubber and synthetic rubber [1]. TPU is a linear block polymer consisting of hard and soft chain segments. Among them, the hard chain segments form a physical cross-linking network with each other, providing TPU with physical properties such as tensile, abrasion and heat resistance. The molecular chains in the soft segments are capable of strong free rotation, providing TPU with excellent elasticity,

similar to rubber [2]. However, TPU is lighter in weight compared to rubber and does not require the vulcanization process necessary for synthetic rubber, so the production process is shortened by 25%, energy consumption is reduced by 25 to 40%, and production efficiency is increased by 10 to 20 times [3]. Therefore, TPU is not only a high-performance, high-quality polymer material but also a friendly material, in line with the requirements of green development [4]. The market demand for TPU has also been increasing in recent years. Its market is estimated to be \$2.3 billion in 2020 and is expected to grow at a

*Corresponding author, e-mail: hhj@jiangnan.edu.cn

© BME-PT

compound annual growth rate of more than 6.5% by 2026 [5].

Traditionally, TPUs are generally processed into products through extrusion, injection moulding, blow moulding, and other moulding processes, mainly used in agriculture, construction, automobiles and daily necessities. However, preparing TPU into nano-scale fiber materials enables it to obtain excellent properties such as high porosity, high surface area, superior mechanical properties and biocompatibility, which are not available in ordinary TPU products, thus could further expand the applicability of TPU in emerging fields of biomedical [6–8], filtration and separation [9–11], and flexible sensing [12–15]. Electrospinning has become the most mature and widely used method to fabricate nanofiber due to the simple technology, low cost, wide variety of spinnable materials and controllable process [16–18]. It works by stretching the spinning solution coming out of the spinneret into nanofibers by means of an auxiliary electrostatic field and then gathering the nanofibers on a grounded collector electrode [19, 20]. The diameter and morphology of the electrospinning nanofibers are of great interest in influencing their mechanical properties. The diameter and morphology of nanofibers depend on many electrospinning parameters that can be classified into four categories: polymer properties (molecular weight and solubility), polymer solution parameters (concentration, viscosity, conductivity and surface tension), processing conditions (applied voltage, collect distance, rotating speed and flow rate) and ambient parameters (temperature, atmosphere pressure, and relative humidity) [21–24]. By optimizing these parameters, not only can nanofibers with homogeneous morphology be obtained, and a quantitative basis for parameters affecting nanofiber diameter and mechanical properties be established, but also time-consuming and excessive experimental costs can be reduced. For experiments on such multivariate problems, response surface methodology (RSM) is the preferred optimization method [25]. Compared with orthogonal experimental design, Taguchi design, full factorial design, and divisional design, RSM can obtain effective information on the factors influencing the dependent variable with fewer trials, and it is suitable for selecting the optimal option from multifactorial and multilevel experiments; thus RSM is efficient and low-cost.

Currently, RSM has been applied to analyze the effect of electrospinning parameters and their interactions on the final performance and the response of mathematical models [26–32]. Eroğlu *et al.* [26] evaluated the correlation between electrospinning parameters (flow rate, applied voltage, polymer/ethanol concentration) and average nanofiber diameter of 2-hydroxyethyl acrylate (pHEMA) by RSM. He *et al.* [27] used RSM to analyze the impacts of process parameters on the diameter and orientation of alternating current electrospun polyacrylonitrile (PAN) nanofibers. Ahmadipourroudposht *et al.* [28] explained the performance of magnetic nanofibers made from polyvinyl alcohol (PVA) and evaluated two important factors, flow rate and applied voltage through RSM. Maleki *et al.* [29] developed an experimental program by the RSM to investigate the influence of electrospinning process parameters on the morphology, diameter and mechanical properties of poly(l-lactide) (PLLA) nanofiber yarns. These fully demonstrate the beneficial role of RSM in the field of optimizing the properties of electrospinning nanofibers. Therefore, RSM can also be considered an effective method to systematically explore the effect of multiple electrospinning parameters on the micromorphology and mechanical properties of TPU nanofibers, thus promoting the development and application of TPU nanomaterials.

Herein, RSM was utilized to predict and verify the diameter of nanofiber with solution concentration, applied voltage, flow rate and rotating speed as key parameters. Then, a linear regression model was established by analysis of variance (ANOVA) to investigate the effects of four spinning parameters on the diameter and microscopic morphology of TPU nanofibers. Further, microscopic characterization and fracture tensile tests were carried out on TPU nanofiber membranes with five concentrations and two orientations to compare their average diameter distributions and investigate their stress-strain properties. Finally, electrospinning parameters with ideal nanofiber diameter and mechanical properties were obtained. This work aims to explore the effect of spinning parameters on the diameter and morphology of TPU nanofibers, which could provide research experience for the subsequent research and development of high-performance TPU nanofibers or the regulation of the nanofiber parameters so that it can be better applied in biomedical, separation and filtration,

flexible sensing and other emerging fields in the future.

2. Experimental section

2.1. Materials

TPU (Elastollan 1185A, $M_w = 30\,000$ g/mol) was purchased from Hongbo Chemical Co., Ltd in Taixing City, China. Reagents *N,N*-dimethylformamide (DMF 99%) used in experiments were provided by China Sinopharm Chemical Reagent Co., Ltd in Shanghai. TPU should be dried at 30 °C for 5 h to remove any possible moisture before the use.

2.2. Preparation of TPU nanofiber membranes

TPU was dissolved in DMF at a certain mass ratio and then magnetically stirred at room temperature, approximately 25±5 °C for 24 h to obtain a homogeneous spinning precursor solution [33]. The solution was placed in a 10 ml syringe with a metal needle (No.19) to set aside. TPU nanofiber membranes were prepared by an electrospinning system (TAKE 602NL, Shanghai, China) consisting of a high voltage supply, syringe, a grounded cylindrical collector,

and temperature and humidity control components, as shown in Figure 1a. The concentration of the spinning solution ranges from 12 to 28 wt%. The flow rate of the polymer solution was set at 1–2 ml/h. 18–28 kV voltage was applied between the needle and the grounded collector to initiate the jet. A collection roller of 7 cm diameter was rotated at 300–700 rpm to collect the nanofibers with a linear speed of 1.1–2.56 m/s [34]. The distance between the rotating drum and the spinneret tip was 12.5 cm. In addition, the electrospinning machine controlled the work conditions with 50±5% RH and a temperature of 25±5 °C. After placing the fiber membrane in Figure 1b, 1c within a fume hood for 24 h to remove residual solvents, it showed excellent ductility (Figure 1d). For convenience, the nanofiber membranes with different solution concentrations are named TPU-X; where X refers to the mass fraction of TPU in the spinning solution. The nanofiber membranes parallel to the collection direction and vertical to the collection direction were labeled as P-TPU and V-TPU, respectively. It can be expressed as P/V-TPU-X when it is necessary to specify both the mass fraction and the orientation of the nanofiber membrane.

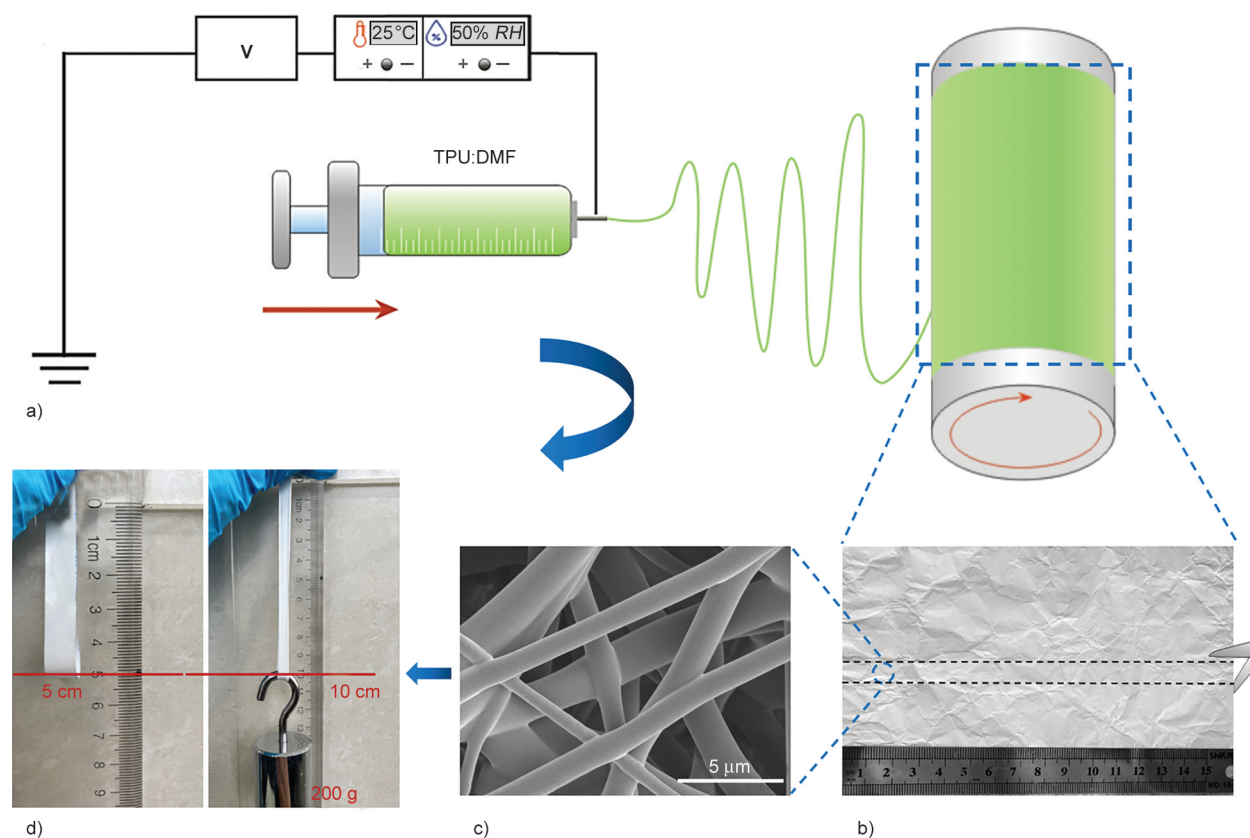


Figure 1. Preparation process of TPU nanofiber membranes. a) Schematic of electrospinning equipment and preparation process. b) Photos of TPU nanofiber membranes. c) FESEM image of the TPU nanofiber. d) The 1×10 cm TPU nanofiber membranes doubled in elongation under the gravity of a 200 g weight.

2.3. Characterization

The surface morphology of the nanofiber membranes was visualized by Field Emission Scanning Electron Microscopy (FESEM, Regulus8100, Tokyo, Japan), as illustrated in Figure 1c. Then the diameters of 100 randomly selected nanofibers from the FESEM images were measured by using ImageJ, followed by a statistical analysis of the mean value of the fiber diameters and the size distribution.

The viscosity of TPU solutions with different mass fractions was determined on a rotary rheometer (Anton Paar Physica MCR301, Graz, Austria) at 25 °C to obtain 50 measurement points. The shear rate is varied logarithmically from 1 to 100 s⁻¹. The distance between the parallel plate and the test bench was 1 mm, the pre-shear rate was set to 10 s⁻¹, and the shear time was 60 s. The operation process is as follows: Firstly, a certain amount of TPU spinning solution was put into the center of the test bench. When the parallel plate was slowly lowered to flatten the TPU spinning stock, the excess TPU spinning stock was scraped off the edge of the parallel plate with a blade, and then the test began.

The stress and strain during stretching were recorded in real-time with a universal material testing machine (5500R Instron, Boston, America). Before the test, all samples were cut into rectangles of 10 mm width and 50 mm length along parallel and vertical directions to the rotation of the collectors. The fiber membranes should be selected where the nanofibers are evenly distributed without areas of excessive accumulation. Then, the samples were fixed with tape in paper frames with a gap size of 1.5×25 mm. The rectangular sample was held by two insulator clamps of the machine, and stretched at a speed of 10 mm/min with an initial gauge length of 25 mm [27]. Hence, the strain rate of the nanofiber membrane in the stretching test is the percentage of the deformation to the initial gauge length. The cross-sectional area of the sample subjected to force is the product of its width and thickness. The thickness of the fiber membranes was measured with a high-precision thickness gauge (resolution 0.001 mm, SYNTEK, Guangzhou, Guangdong).

2.4. Design of experiments

To investigate the influence of four processing parameters (solution concentration, applied voltage, flow rate and rotating speed) on TPU nanofiber diameter and microscopic morphology, a three-level

Box-Behnken Design was applied for four independent variables by Design Expert. The spinning parameters (*i.e.*, the solution concentration of 12, 20, 28 wt%, applied voltage of 18, 23, 28 kV, flow rate of 1, 1.5, 2 ml/h, rotating speed of 300, 500, 700 rpm) were selected based on literature [35, 36]. Thus, 29 sets of nanofiber membrane preparation experiments were carried out. Then “RSM” was employed to optimize, model and analyze the performance of TPU nanofiber. The responses (nanofiber diameters) were evaluated and analyzed according to experimental independent factors (processing parameters). A quadratic regression model was used to describe the relationship between important input factors and measurable output (Equation (1)). The full factorial design matrix is shown in Table 1:

Table 1. The Box-Behnken Design for TPU electrospinning involved four parameters with three levels.

Sample number	TPU concentration [wt%]	Applied voltage [kV]	Flow rate [ml/h]	Rotating speed [rpm]
1	20	28	1.5	700
2	28	23	1.5	700
3	28	28	1.5	500
4	20	23	2.0	700
5	20	23	1.0	300
6	20	23	1.5	500
7	20	18	2.0	500
8	28	23	2.0	500
9	20	18	1.5	700
10	20	28	1.0	500
11	20	28	1.5	300
12	20	23	2.0	300
13	28	23	1.5	300
14	12	28	1.5	500
15	20	28	2.0	500
16	20	18	1.0	500
17	20	23	1.0	700
18	12	23	1.5	700
19	20	23	1.5	500
20	20	18	1.5	300
21	12	18	1.5	500
22	12	28	1.0	700
23	12	23	2.0	500
24	20	23	1.5	500
25	28	23	1.0	500
26	20	23	1.5	500
27	20	23	1.5	500
28	28	18	1.5	500
29	12	23	1.5	300

$$y = \beta_0 + \sum_{i=1}^k \beta_i x_i + \sum_{i=1}^k \beta_{ii} x_i^2 + \sum_{i < j} \beta_{ij} x_i x_j + \varepsilon \quad (1)$$

where y is the response; β_0 , β_i , β_{ii} and β_{ij} are the regression coefficients to be determined; k represents the number of the independent variables “ x_i ”, and “ ε ” is the statistical error.

3. Results and discussion

3.1. Importance evaluation of the electrospinning parameters

The maximum and minimum of average nanofiber diameters were obtained from Sample 1 and Sample 22 with 1.45 ± 0.46 and 0.16 ± 0.05 μm , respectively (Figure 2). There were a plenty of beaded fibers in Sample 22 (about 160 beads in Figure 2a at $1000\times$ magnification) due to the low solution concentration (12 wt%). In contrast, the nanofiber morphology of Sample 1 in Figure 2b and Figure 2b' was more homogeneous and average nanofiber diameter was larger (1.45 μm). Whereas, spindle-shaped nanofibers appeared in Sample 3 with the highest solution concentration (28 wt%), spinning voltage (28 kV) and flow rate (1.5 ml/h) (in Figure 2c and Figure 2c').

Without any transformation in data, the results of all 29 experimental groups were selected to perform the

analysis of variance (ANOVA) [28]. The result of the ANOVA was summarized in Table 2 to estimate the impact of four spinning parameters on nanofiber diameter [26], including the p -value, coefficient of determination (R^2), adjusted R^2 and adequate precision. Each coefficient's importance was determined by p -values. The factor can be indicated as the most significant factor when their p -values are <0.05 . While the p -value for the model is <0.0001 , indicating that the model is considered statistically significant [37]. It is obvious that solution concentration (X_1) was determined as a significant model term but coefficients of applied voltage (X_2), flow rate (X_2) and rotating speed (X_3) are found to be insignificant. The coefficient of determination (R^2) is used for the goodness of the fit with the model and should be close to desirable 1. The R^2 of this model was determined as 95.26%, indicating that only 4.76% of all the variables are out of the regression model, which proved that the model agrees well with experimental results. Moreover, the coefficient of adjusted R^2 (90.52%) also greatly illustrated the significance of the model. The adequate precision (12.946) is greater than 4 [28, 38], also suggesting that the accuracy and the ratio of the model are desirable. The relationship between the processing parameters and nanofiber diameter obtained from the ANOVA analysis is shown in Equation (2):

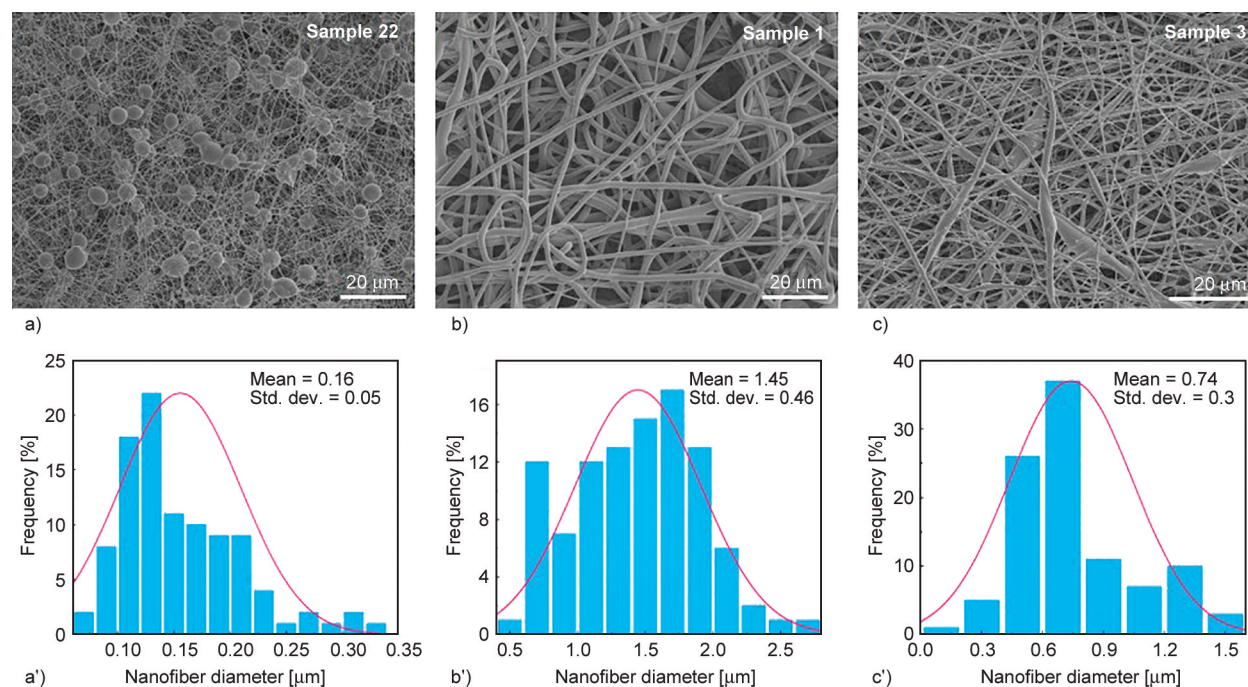


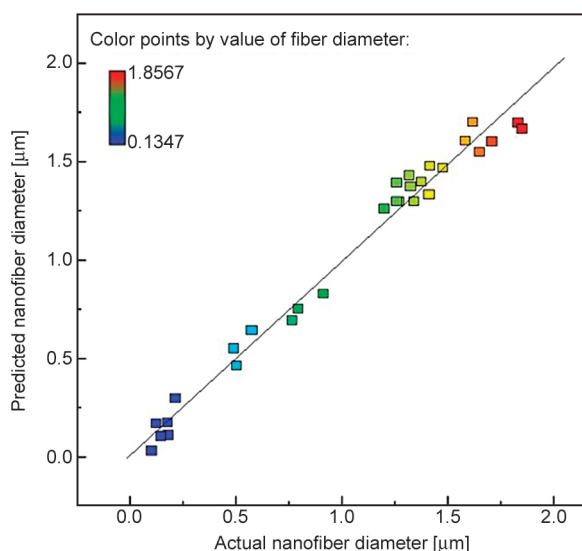
Figure 2. The microscopic morphology and diameter distribution of three groups' nanofibers: a) and a') Sample 22, b) and b') Sample 1, c) and c') Sample 3.

Table 2. ANOVA test results for estimation of minimum nanofiber diameter.

Source	Sum of squares	DF	Mean square	F-value	p-value
Model	8.87	14	0.63	20.10	<0.0001
X_1 -TPU concentration	0.70	1	0.70	22.28	0.0003
X_2 -applied voltage	0.055	1	0.055	1.75	0.207
X_3 -flow rate	$4.92 \cdot 10^{-3}$	1	$4.92 \cdot 10^{-3}$	0.16	0.6987
X_4 -rotating speed	0.043	1	0.043	1.36	0.2627
X_1X_2	0.039	1	0.039	1.24	0.2844
X_1X_3	0.012	1	0.012	0.38	0.5486
X_1X_4	0.023	1	0.023	0.74	0.4034
X_2X_3	$3.45 \cdot 10^{-4}$	1	$3.45 \cdot 10^{-4}$	0.011	0.9181
X_2X_4	0.028	1	0.028	0.87	0.3659
X_3X_4	$1.91 \cdot 10^{-4}$	1	$1.91 \cdot 10^{-4}$	$6.07 \cdot 10^{-3}$	0.9390
X_1^2	6.420	1	6.420	203.72	<0.0001
X_2^2	0.067	1	0.067	2.12	0.1677
X_3^2	0.019	1	0.019	0.59	0.4539
X_4^2	0.270	1	0.270	8.45	0.0115
R^2	95.26%				
Adjusted R^2	90.52%				
Adequate precision	12.946				

$$\begin{aligned}
 Y_{\text{Average nanofiber diameter}} &= \\
 &= 1.28 + 0.24X_1 + 0.068X_2 - 0.02X_3 + 0.06X_4 + \\
 &+ 0.099X_1X_2 + 0.055X_1X_3 - 0.076X_1X_4 - \\
 &- 0.00929X_2X_3 - 0.083X_2X_4 + 0.00691X_3X_4 - \\
 &- 0.99X_1^2 + 0.1X_2^2 + 0.054X_3^2 + 0.2X_4^2
 \end{aligned} \quad (2)$$

To verify the model's accuracy, predicted and actual response values were evaluated. Figure 3 presents that the predicted nanofiber diameters are in good agreement with the actual nanofiber diameter. With this model, the influence of the single parameters on the microscopic morphology of the nanofibers was evaluated, as depicted in Figure 4. Among them, concentration had the most significant effect on nanofiber diameter because the slope of the curve is the largest. As illustrated in Figure 4a, the nanofiber diameter showed a tendency to increase and then decrease as the solution concentration increased. The reason for this is that a minimum solution concentration is required for the solution to form a Taylor cone and further to be drawn into nanofibers during electrospinning. Below this concentration, the surface tension of the spinning solution is insufficient, and the degree of polymer chain entanglement cannot resist the electric field force, resulting in the formation of bead-like fibers, *i.e.*, mixtures of polymer particles and finer nanofibers as the jet breaks during the spinning process (Figure 2a and Figure 2a'). The spinning solution with appropriate concentration

**Figure 3.** The predicted nanofiber diameter and the actual nanofiber diameter.

facilitates the entanglement of molecular chains, so the jet is not easy to break, which can form a uniform and regular nanofibers under the full stretching by electric field force (Figure 2b and Figure 2b') [39, 40]. Once the solution concentration exceeds the limit, it will cause the solution to accumulate in the nozzle so that a stable jet stream cannot be formed, and the sprayed solution will also tend to aggregate into spindle-shaped nanofibers, as indicated in Figure 2c. However, a small portion of the outer edge of the jet can be stretched out and extended very thinly under a strong electric field, causing a

decrease in the overall nanofiber diameter except for the spindle-shaped nanofibers (Figure 2c').

Compared to the solution concentration, we found that the effect of applied voltage in Figure 4b is more monotonous. If the voltage is too low, the electrical force may not be sufficient to stretch the polymer solution into fine nanofibers. When the voltage is too high, excessive stretching may reduce the diameter of the nanofibers and even damage the continuous polymer jet. The effect of flow rate on the diameter of nanofibers in Figure 4c is also unremarkable. The higher the flow rate and the more spinning solution ejected at the same time, the thicker the nanofibers will be. However, if the flow rate is too small, the nanofibers will become finer and may break due to excessive stretching. Besides, rotating speed has a similar influence on nanofiber diameter as voltage, as can be seen in Figure 4d. A slow rotating speed is not sufficient to stretch nanofiber, while a faster speed will cause the polymer jets to break due to

electric field forces. Therefore, the finest nanofibers can only be prepared at the suitable electrospinning parameters.

It was verified by 29 sets of orthogonal tests that the most influential factor on nanofiber morphology was concentration. Next, further experiments were carried out with a gradient variable with a concentration of 3 wt% based on the parameters of group 22 (20 wt%, 28 kV, 1 ml/h and 700 rpm) that had the smallest fiber diameter and the best morphology.

3.2. Effect of the concentration on the diameter of TPU nanofibers

To further explore the most suitable TPU electrospinning concentration, we conducted additional experiments to analyze the nanofiber morphology and diameter at spinning solution concentrations ranging from 14 to 26% (3 wt% gradient). The single-factor experimental design is shown in Table 3. It can be seen in Figure 5a–5e that the surface of TPU

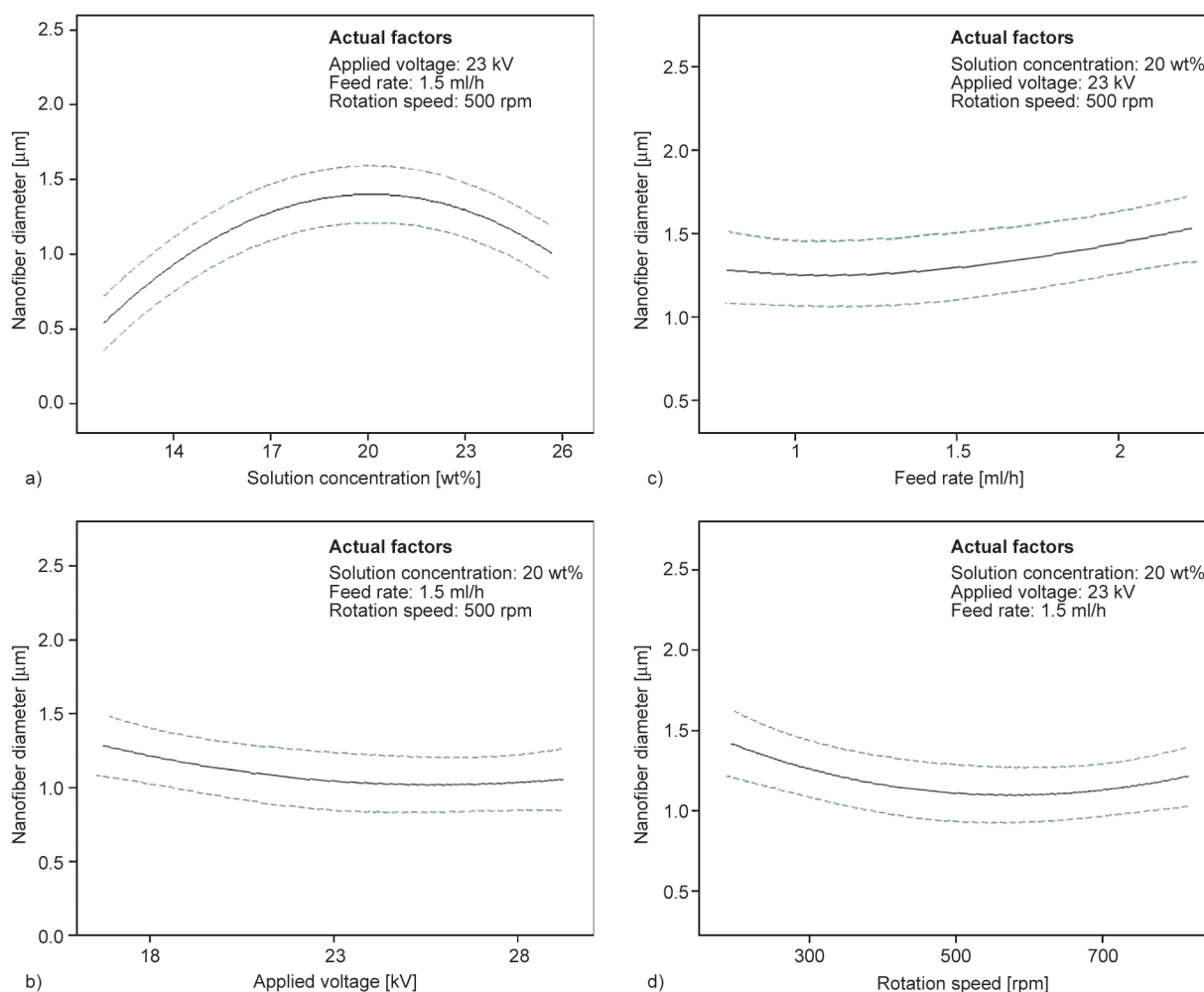


Figure 4. The predicted relationship between single processing parameters and nanofiber diameter in the model: a) solution concentration, b) applied voltage, c) flow rate, d) rotating speed.

Table 3. Single factor experimental design of spinning solution concentration.

Sample number	TPU concentration [wt%]	Fiber diameter [μm]
1	23	1.46
2	26	1.47
3	17	0.69
4	20	1.25
5	14	0.35
6	14	0.37
7	26	1.47

nanofiber membranes showed a uniform mesh structure without droplets and spindle-shaped fibers when the concentration was in the range of 14 to 26 wt%, indicating that the concentration range was suitable for electrospinning of TPU. However, the nanofiber diameter gradually expanded from $0.36\pm 0.11\ \mu\text{m}$ (14 wt%) to $1.47\pm 0.35\ \mu\text{m}$ (26 wt%) with the increase of concentration, as depicted in Figure 5a'–5e' and Figure 5f. The reason is that the appropriate viscoelastic resistance of the solution, as well as the degree of entanglement of the molecular chains and inter-chain friction, make it easier to stretch the intermolecular chain segments into filaments within the appropriate concentration range of the spinning solution, resulting in a higher degree of nanofiber continuity. Figure 6 shows the viscosity

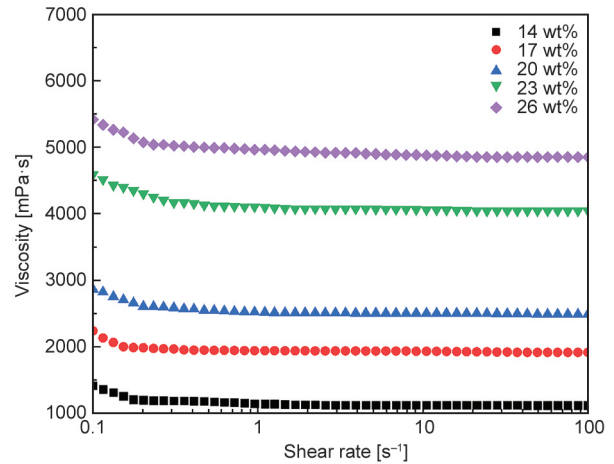


Figure 6. Viscosity of TPU electrospinning solutions.

of five concentrations of TPU solutions against the shear rate of $0.1\text{--}100\ \text{s}^{-1}$. The viscosity of the solution increases with increasing TPU content due to its high molecular weight. However, lower solution viscosity will contribute to less viscoelastic resistance, and the nanofibers will be fully stretched under the electric field, resulting in finer diameters and worse stability. Higher solution viscosity is accompanied by higher viscoelastic resistance, which can result in coarser nanofibers that are not sufficiently stretched by the electric field. Both of these conditions will lead to an uneven distribution of nanofiber diameters.

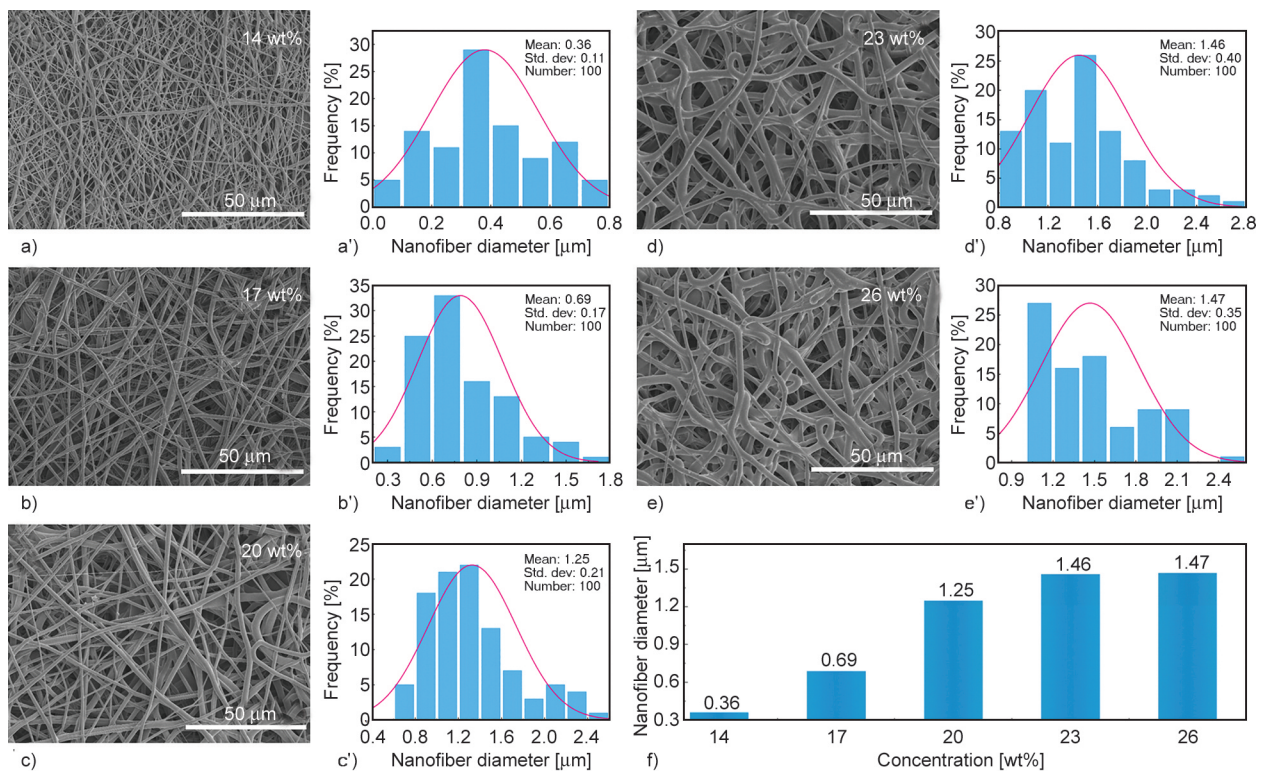


Figure 5. a)–e) FESEM images and diameter distribution of nanofibers at five concentrations. f) The average nanofiber diameter increased with solution concentration.

Based on the FESEM images and diameter distribution statistics in Figure 5, it can be concluded that 20 wt% of the nanofibers have a more uniform nanofiber diameter, indicating a suitable viscoelasticity at this concentration. Consequently, it is obvious that a 20 wt% mass fraction of spinning solution at 28 kV, a flow rate of 1 ml/h and a rotating speed of 700 rpm was able to obtain the most homogeneous TPU nanofiber with high porosity (mean is 1.25 μm , standard deviation is 0.21).

3.3. Effect of concentration and orientation on the mechanical properties of TPU nanofiber membranes

Furthermore, the mechanical properties of the nanofibers varied with the concentration of the spinning solution and showed different characteristics in parallel and vertical orientations. To further investigate the mechanical properties of TPU nanofiber membranes with different proportions, a series of monotonic tensile tests were performed. Figure 7a and Figure 7b shows the typical stress-strain variation of TPU fiber membranes in the parallel direction. Apparently, the stress and strain of P-TPU nanofiber membranes tended to increase and then decrease with increasing concentration. Among them, the mechanical properties of P-TPU-20 were optimal,

with 411% elongation at break and 23.71 MPa stress strength. These are due to the fact that the more uniform the arrangement and diameter of the nanofibers are at the optimal spinning solution concentration, the more stable the stress transfer during stretching is and the greater the stress and strain can be withstood. Figure 7d and Figure 7e shows the mechanical properties of the nanofiber membrane vertical to the collection direction. It can be seen that the trends of elongation and breaking strength of V-TPU nanofiber membranes are similar to those of P-TPU, where V-TPU-20 still exhibits optimal mechanical performance. It was confirmed again that nanofibers at a concentration of 20 wt% with better alignment provided higher strain and tensile strength.

Obviously, P-TPU-20 nanofiber membranes (23.71 MPa) exhibited stronger stress than V-TPU-20 nanofiber membranes (17.81 MPa), while the breaking elongation of V-TPU-20 nanofiber membranes (485%) was about 1.2 times that of P-TPU-20 nanofiber membranes (411%), superior to related literature [34, 35]. The favorable strain performance was mainly related to the orientation of nanofibers when they were collected from the rotating collector. The rapid rotation of the collection rollers caused the nanofibers to align with the direction of rotation, resulting in the anisotropy of the nanofiber membrane,

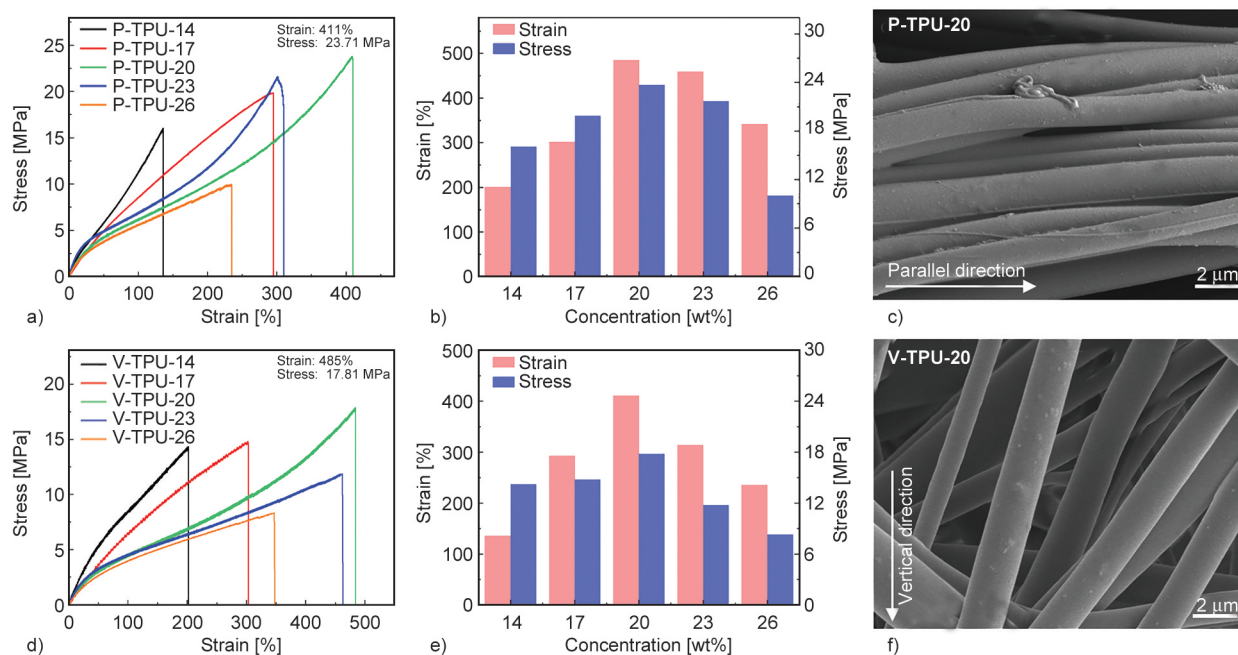


Figure 7. Mechanical properties of TPU nanofiber membranes in parallel and vertical orientation. a), b) Stress-strain at break and mechanical properties of the TPU nanofiber membrane at five concentrations in the parallel direction. c) The FESEM images of P-TPU-20. d), e) Stress-strain at break and mechanical properties of the TPU nanofiber membrane at five concentrations in the vertical direction. f) The FESEM images of V-TPU-20.

as displayed in Figure 7c and Figure 7f. Along the parallel direction, the nanofiber will be directly straightened under stretching and deformed by its own elasticity. When the force is applied along the vertical direction, the pores in the nanofiber network will first be stretched wider and then continue to elongate through their own elasticity, meaning that these fishing net-like gaps widen the strain range. As a result, the V-TPU nanofiber membrane exhibits a weak dependence of stress on strain due to the deformation of the gap, providing a wider strain response range and more outstanding repeatability and recoverability than the P-TPU nanofiber membrane. To summarize, spinning solution concentration has a significant effect on nanofiber morphology and mechanical properties. By using the process parameters selected from RSM, TPU nanofibers with uniform morphology and finer diameter can be obtained without forming any bead or spindle shape. Nanofibers with optimum solution concentration (20 wt%) have a more desirable stress intensity and strain range. The strain range of the nanofiber membrane vertical to the collection direction is larger than that parallel to it, but the stress intensity is the opposite. Benefiting from the RSM, the nanofiber diameter can be predicted from known electrospinning parameters by Equation (2), and the mechanical properties of the nanofiber membrane can be adjusted by controlling the collection direction. However, it is notable that different experimental conditions and raw materials may lead to varying experimental results. Therefore, the electrospinning fabrication of TPU needs further standardization.

4. Conclusions

In this study, RSM was used to investigate the influence of four processing parameters on the performances (*i.e.*, nanofiber morphology, diameter and mechanical performance) of nanofibers with the aim of optimizing the preparation process of TPU nanofibers in order to save the cost of time, material and labor. The ANOVA of 29 sets of experiments showed that among the four spinning parameters, solution concentration had the most significant effect on nanofiber diameter. The finest nanofiber diameters with the most uniform and homogeneous structures were obtained from 20 wt% (applied voltage of 28 kV, flow rate of 1 ml/h and rotating speed of 700 rpm). We also compared the mechanical properties of the samples in vertical and parallel directions.

The nanofibers in the parallel direction showed the highest stress (23.71 MPa) due to the stress concentration. While the nanofibers in the vertical direction demonstrated a larger strain range (485%) owing to the lateral deformation of the nanofiber network. It is noteworthy that this study will provide useful guidance for future research on the preparation of TPU nanofibers and related applications.

Acknowledgements

This research was funded by the National Science Foundation (52303054), Natural Science Foundation of Jiangsu Province (BK20221094, BK20231056), the fellowship of China Postdoctoral Science Foundation (2022TQ0123), the Fundamental Research Funds for the Central Universities (JUSRP122003, JUSRP123005), “Taihuzhiguang” Science and Technology Research (fundamental research) Project of Wuxi (K20221007) and Postgraduate Research & Practice Innovation Program of Jiangsu Province (KYCX22_2350).

References

- [1] Oksman K., Lindberg H.: Influence of thermoplastic elastomers on adhesion in polyethylene-wood flour composites. *Journal of Applied Polymer Science*, **68**, 1845–1855 (1998).
[https://doi.org/10.1002/\(sici\)1097-4628\(19980613\)68:11<1845::aid-app16>3.0.co;2-t](https://doi.org/10.1002/(sici)1097-4628(19980613)68:11<1845::aid-app16>3.0.co;2-t)
- [2] Yao Y., Xiao M., Liu W. G.: A short review on self-healing thermoplastic polyurethanes. *Macromolecular Chemistry and Physics*, **222**, 202100002 (2021).
<https://doi.org/10.1002/macp.202100002>
- [3] Datta J., Kasprzyk P.: Thermoplastic polyurethanes derived from petrochemical or renewable resources: A comprehensive review. *Polymer Engineering and Science*, **58**, E14–E35 (2018).
<https://doi.org/10.1002/pen.24633>
- [4] Khalifa M., Anandhan S., Wuzella G., Lammer H., Mahendran A. R.: Thermoplastic polyurethane composites reinforced with renewable and sustainable fillers – A review. *Polymer-Plastics Technology and Materials*, **59**, 1751–1769 (2020).
<https://doi.org/10.1080/25740881.2020.1768544>
- [5] Backes E. H., Harb S. V., Pinto L. A., de Moura N. K., de Melo Morgado G. F., Marini J., Passador F. R., Pessan L. A.: Thermoplastic polyurethanes: Synthesis, fabrication techniques, blends, composites, and applications. *Journal of Materials Science*, **59**, 1123–1152 (2024).
<https://doi.org/10.1007/s10853-023-09077-z>
- [6] Liu N-H., Pan J-F., Miao Y-E., Liu T-X., Xu F., Sun H.: Electrospinning of poly(ϵ -caprolactone-*co*-lactide)/pluronic blended scaffolds for skin tissue engineering. *Journal of Materials Science*, **49**, 7253–7262 (2014).
<https://doi.org/10.1007/s10853-014-8432-8>

- [7] Goyal R., Marci L. K., Kaplan H. M., Kohn J.: Nanoparticles and nanofibers for topical drug delivery. *Journal of Controlled Release*, **240**, 77–92 (2016).
<https://doi.org/10.1016/j.jconrel.2015.10.049>
- [8] Gao W-C., Wu W., Chen C-Z., Zhao H., Liu Y., Li Q., Huang C-X., Hu G-H., Wang S-F., Shi D., Zhang Q-C.: Design of a superhydrophobic strain sensor with a multilayer structure for human motion monitoring. *ACS Applied Materials and Interfaces*, **14**, 1874–1884 (2021).
<https://doi.org/10.1021/acsami.1c17565>
- [9] Qin X-H., Wang S-Y.: Filtration properties of electrospinning nanofibers. *Journal of Applied Polymer Science*, **102**, 1285–1290 (2006).
<https://doi.org/10.1002/app.24361>
- [10] Zhu M., Han J., Wang F., Shao W., Xiong R., Zhang Q., Pan H., Yang Y., Samal S. K., Zhang F., Huang C.: Electrospun nanofibers membranes for effective air filtration. *Macromolecular Materials and Engineering*, **302**, 1600353 (2016).
<https://doi.org/10.1002/mame.201600353>
- [11] Li Z., Wang S., Wen Y., Sun X., Cao B., Kang W., Liu Y.: A nanofiber Murray membrane with antibacterial properties for high efficiency oily particulate filtration. *European Polymer Journal*, **191**, 112036 (2023).
<https://doi.org/10.1016/j.eurpolymj.2023.112036>
- [12] Zhang L., Jiang F., Wang L., Feng Y., Yu D., Yang T., Wu M., Petru M.: High performance flexible strain sensors based on silver nanowires/thermoplastic polyurethane composites for wearable devices. *Applied Composite Materials*, **29**, 1621–1636 (2022).
<https://doi.org/10.1007/s10443-022-10029-0>
- [13] Kang L., Ma J., Wang C., Li K., Wu H., Zhu M.: Highly sensitive and wide detection range thermoplastic polyurethane/graphene nanoplatelets multifunctional strain sensor with a porous and crimped network structure. *ACS Applied Materials and Interfaces*, **16**, 2814–2824 (2024).
<https://doi.org/10.1021/acsami.3c18397>
- [14] Chung M., Skinner W. H., Robert C., Campbell C. J., Rossi R. M., Koutsos V., Radacsi N.: Fabrication of a wearable flexible sweat pH sensor based on SERS-Active Au/TPU electrospun nanofibers. *ACS Applied Materials and Interfaces*, **13**, 51504–51518 (2021).
<https://doi.org/10.1021/acsami.1c15238>
- [15] Liu L., Luo T., Kuang X., Wan X., Liang X., Jiang G., Cong H., He H.: Highly stretchable and multimodal MXene/CNTs/TPU Flexible resistive sensor with hierarchical structure inspired by annual ring for hand rehabilitation. *ACS Sensors*, in press (2024).
<https://doi.org/10.1021/acssensors.4c00164>
- [16] Keirouz A., Wang Z., Reddy V. S., Nagy Zs. K., Vass P., Buzgo M., Ramakrishna S., Radacsi N.: The history of electrospinning: Past, present, and future developments. *Advanced Materials Technologies*, **8**, 2201723 (2023).
<https://doi.org/10.1002/admt.202201723>
- [17] Kenry N., Lim C. T.: Nanofiber technology: Current status and emerging developments. *Progress in Polymer Science*, **70**, 1–17 (2017).
<https://doi.org/10.1016/j.progpolymsci.2017.03.002>
- [18] Bhardwaj N., Kundu S. C.: Electrospinning: A fascinating fiber fabrication technique. *Biotechnology Advances*, **28**, 325–347 (2010).
<https://doi.org/10.1016/j.biotechadv.2010.01.004>
- [19] Ghosh T., Das T., Purwar R.: Review of electrospun hydrogel nanofiber system: Synthesis, properties and applications. *Polymer Engineering and Science*, **61**, 1887–1911 (2021).
<https://doi.org/10.1002/pen.25709>
- [20] Barhoum A., Pal K., Rahier H., Uludag H., Kim I. S., Bechelany M.: Nanofibers as new-generation materials: From spinning and nano-spinning fabrication techniques to emerging applications. *Applied Materials Today*, **17**, 1–35 (2019).
<https://doi.org/10.1016/j.apmt.2019.06.015>
- [21] Sun G., Sun L., Xie, H., Liu J.: Electrospinning of nanofibers for energy applications. *Nanomaterials*, **6**, 129 (2016).
<https://doi.org/10.3390/nano6070129>
- [22] Shahriar S. S. M., Mondal J., Hasan M. N., Revuri V., Lee D. Y., Lee Y-K.: Electrospinning nanofibers for therapeutics delivery. *Nanomaterials*, **9**, 532 (2019).
<https://doi.org/10.3390/nano9040532>
- [23] Liu S., White K. L., Reneker D. H.: Electrospinning polymer nanofibers with controlled diameters. *IEEE Transactions on Industry Applications*, **55**, 5239–5243 (2019).
<https://doi.org/10.1109/tia.2019.2920811>
- [24] Nasouri K., Bahrambeygi H., Rabbi A., Shoushtari A. M., Kafrou A.: Modeling and optimization of electrospun PAN nanofiber diameter using response surface methodology and artificial neural networks. *Journal of Applied Polymer Science*, **126**, 127–135 (2012).
<https://doi.org/10.1002/app.3672>
- [25] Dayan C. B., Afghah F., Okan B. S., Yildiz M., Menciloglu Y., Culha M., Koc B.: Modeling 3D melt electrospinning writing by response surface methodology. *Materials and Design*, **148**, 87–95 (2018).
<https://doi.org/10.1016/j.matdes.2018.03.053>
- [26] Eroğlu A. N., Aydın R. S. T., Karakeçili A., Çalimli A.: Fabrication and process optimization of poly(2-hydroxyethyl methacrylate) nanofibers by response surface methodology. *Journal of Nanoscience and Nanotechnology*, **17**, 616–625 (2017).
<https://doi.org/10.1166/jnn.2017.12806>
- [27] He H., Wang Y., Farkas B., Nagy Zs. K., Molnár K.: Analysis and prediction of the diameter and orientation of AC electrospun nanofibers by response surface methodology. *Materials and Design*, **194**, 108902 (2020).
<https://doi.org/10.1016/j.matdes.2020.108902>

- [28] Ahmadipourroudosht M., Fallahiarezoudar E., Yusof N. M., Idris A.: Application of response surface methodology in optimization of electrospinning process to fabricate (ferrofluid/polyvinyl alcohol) magnetic nanofibers. *Materials Science and Engineering C-materials For Biological Applications*, **50**, 234–241 (2015).
<https://doi.org/10.1016/j.msec.2015.02.008>
- [29] Maleki H., Gharehaghaji A. A., Criscenti G., Moroni L., Dijkstra P. J.: The influence of process parameters on the properties of electrospun PLLA yarns studied by the response surface methodology. *The Journal of Applied Polymer Science*, **132**, 41388 (2014).
<https://doi.org/10.1002/app.41388>
- [30] Boaretti C., Roso M., Lorenzetti A., Modesti M.: Synthesis and process optimization of electrospun PEEK-sulfonated nanofibers by response surface methodology. *Materials*, **8**, 4096–4117 (2015).
<https://doi.org/10.3390/ma8074096>
- [31] Agarwal P., Mishra P. K., Srivastava P.: Statistical optimization of the electrospinning process for chitosan/poly lactide nanofabrication using response surface methodology. *Journal of Materials Science*, **47**, 4262–4269 (2012).
<https://doi.org/10.1007/s10853-012-6276-7>
- [32] Padmanabhan T., Kamaraj V., Magwood L., Starly B.: Experimental investigation on the operating variables of a near-field electrospinning process *via* response surface methodology. *Journal of Manufacturing and Materials Processing*, **13**, 104–112 (2011).
<https://doi.org/10.1016/j.jmapro.2011.01.003>
- [33] Wei L., Qiu Q., Wang R., Qin X.: Influence of the processing parameters on needleless electrospinning from double ring slits spinneret using response surface methodology. *Journal of Applied Polymer Science*, **50**, 234–241 (2018).
<https://doi.org/10.1002/app.46407>
- [34] Chen Y., Wang N., Jensen M., Li X. F.: Low-temperature welded PAN/TPU composite nanofiber membranes for water filtration. *Journal of Water Process Engineering*, **47**, 102806 (2022).
<https://doi.org/10.1016/j.jwpe.2022.102806>
- [35] Wang X., Liu X., Schubert D. W.: Highly sensitive ultrathin flexible thermoplastic polyurethane/carbon black fibrous film strain sensor with adjustable scaffold networks. *Nano-Micro Letters*, **13**, 64 (2021).
<https://doi.org/10.1007/s40820-021-00592-9>
- [36] Xia Y., He L., Feng J., Xu S., Yao L., Pan G.: Waterproof and moisture-permeable polyurethane nanofiber membrane with high strength, launderability, and durable antimicrobial properties. *Nanomaterials*, **12**, 1813 (2022).
<https://doi.org/10.3390/nano12111813>
- [37] Megelski S., Stephens J. S., Chase D. B., Rabolt J. F.: Micro- and nanostructured surface morphology on electrospun polymer fibers. *Macromolecules*, **35**, 8456–8466 (2002).
<https://doi.org/10.1021/ma020444a>
- [38] Jensen W. A.: Design and analysis of experiments by Douglas Montgomery: A supplement for using JMP. *Journal of Quality Technology*, **46**, 181–182 (2014).
<https://doi.org/10.1080/00224065.2014.11917962>
- [39] Molnár K., Nagy Zs. K.: Corona-electrospinning: Needleless method for high-throughput continuous nanofiber production. *European Polymer Journal*, **74**, 279–286 (2016).
<https://doi.org/10.1016/j.eurpolymj.2015.11.028>
- [40] He H., Kara Y., Molnár K.: *In situ* viscosity-controlled electrospinning with a low threshold voltage. *Macromolecular Materials and Engineering*, **304**, 1900349 (2019).
<https://doi.org/10.1002/mame.201900349>